University of Nevada, Reno

Organic Ionic Salt Draw Solutions for Osmotic Membrane Bioreactors

A thesis submitted in partial fulfillment of the requirements for the degree of Master of Science in Civil and Environmental Engineering

By

Katie S. Bowden

Dr. Amy E. Childress/Thesis Advisor

December, 2012

University of Nevada, Reno
Statewide • Worldwide

THE GRADUATE SCHOOL

We recommend that the thesis
prepared under our supervision by

KATIE S. BOWDEN

entitled

Organic Ionic Salt Draw Solutions For Osmotic Membrane Bioreactors

be accepted in partial fulfillment of the
requirements for the degree of

MASTER OF SCIENCE

Amy E. Childress, Ph.D., Advisor

Eric A. Marchand, Ph.D., Committee Member

Andrea Achilli, Ph.D., Committee Member

Dev Chidambaram, Ph.D., Graduate School Representative

Marsha H. Read, Ph. D., Dean, Graduate School

December, 2012

ABSTRACT

This investigation evaluates the use of organic ionic salt solutions as draw solutions for specific use in osmotic membrane bioreactors. The osmotic membrane bioreactor is an innovative system, representing a combination of forward osmosis and membrane bioreactor technology to improve the quality of wastewater effluent for potable reuse applications. Selecting an optimal draw solution for forward osmosis applications is imperative for efficient system performance. A selection of organic ionic draw solutions underwent a desktop screening process before being tested in the laboratory and evaluated for performance using specific salt flux (reverse salt flux per unit water flux), biodegradation potential, and cost. All of the salts tested have organic anions with the potential to be degraded in the bioreactor as a carbon source and aid in nutrient removal. Two of the salts (sodium propionate and magnesium acetate) were found to have specific salt fluxes three to six times lower than two commonly used inorganic draw solutions, NaCl and $MgCl_2$. Magnesium acetate had the lowest specific salt flux, indicating the highest process efficiency, but also required the most salt to achieve desired osmotic pressures, contributing to higher costs than sodium propionate. Sodium propionate was tested in batch biological experiments; it found to increase the rate of denitrification in an anoxic environment and to degrade completely in an aerobic environment. Thus, sodium propionate appears to be a highly suitable draw solution for osmotic membrane bioreactor systems.

Keywords: Organic draw solution, Draw solution, Osmosis, Forward osmosis, Osmotic membrane bioreactor, Membrane bioreactor, Reverse salt flux, Denitrification, Potable reuse

ACKNOWLEDGEMENTS

I would like to express my thanks to my advisor, Dr. Amy Childress, for her efforts and commitment to my success and that of all her students. I'm very grateful for the instruction and advisement that have prepared me for all types of future endeavors and challenges.

I would also like to thank my committee members, Dr. Eric Marchand, Dr. Dev Chidambaram, and Dr. Andrea Achilli for their time and feedback. I realize how busy their schedules are and want to express my gratitude to them for dedicating the time required by this commitment.

Special thanks to Mark Lattin for having no limits to the problems he will take on and solve, no matter the time of the day or day of the week. I especially appreciate the extensive time spent by Mark and Zach Linde working with LabVIEW.

I couldn't have completed this project without the collaboration with and assistance from past and present members of the Childress research group and fellow environmental engineering students and staff: Andrea, Sage, Jeff, Jeri, Guiying, Ally, Emily C., Wes, Tony, Viktoriya, Pawel, Jahid, and Nick. A big thanks to the lifesaver who helped me on every hectic day of running experiments, Emily R.

The generous support for this project was provided by the Environmental Protection Agency (EPA) through the EPA Star Graduate Fellowship program as well as the Nevada NASA Space Grant Consortium for fellowship funding.

TABLE OF CONTENTS

Abstract……i

Acknowledgements……ii

Table of Contents……iii

List of Acronyms……v

List of Tables……..vi

List of Figures……vii

1. Introduction……1

2. Theory……6

3. Materials and Methods……..11

3.1 Desktop Screening Process……..12

3.2 FO Experiments……...14

3.2.1 Membranes……14

3.2.2 Solution chemistries……...14

3.2.3 Laboratory testing apparatus……..15

3.2.4 FO testing procedure……..17

3.3 RO experiments……...19

3.3.1 Membranes……19

3.3.2 Solution chemistries……..19

3.3.3 Laboratory testing apparatus……19

3.3.4 Testing procedure……..20

3.4 Biodegradation quantification……20

3.4.1 Prediction of biological performance……20

3.4.2 Batch biological experiments……21

3.5 Replenishment cost determination……...24

4. Results and Discussion…….25

4.1 Water flux……....25

4.2 Reverse salt flux……...26

4.3 Specific salt flux……..28

4.4 RO Reconcentration…….30

4.5 Biodegradation of draw solutions……31

4.5.1 Prediction of biological performance ……31

4.5.2 Batch biological experiments…….32

4.6 Replenishment cost……..38

4.7 Future Work…….39

5. Conclusions……...40

References……..41

LIST OF ACRONYMS

FO	Forward osmosis
OMBR	Osmotic membrane bioreactor
MBR	Membrane bioreactor
RO	Reverse osmosis
MD	Membrane distillation
D	Diffusion coefficient
HRT	Hydraulic retention time
SRT	Solids retention time
C/N	Carbon-to-nitrogen
ECP	External concentration polarization
ICP	Internal concentration polarization
HMIS	Hazardous materials identification system
CTA	Cellulose triacetate

LIST OF TABLES

Table 1. Draw solution unit costs, specific costs, and osmotic pressures achieved at saturation concentration.

Table 2. Aqueous solution osmotic pressure (π_{DS}), concentration (C_{DS}), water flux (J_w), solute resistivity (K), and diffusion coefficient (D) for each draw solution.

Table 3. Aqueous solution osmotic pressure (π_{DS}), concentration (C_{DS}), reverse salt flux (J_s), water flux (J_w), effective osmotic pressure ($\pi_{D,i}$), effective draw solution concentration ($C_{D,i}$), and specific reverse salt flux (J_s/J_w). $\pi_{D,i}$ was calculated using Eq. (8) and the corresponding $C_{D,i}$ was calculated using OLI Stream Analyzer™.

Table 4. Draw solution concentrations corresponding to an osmotic pressure of 1.4 MPa, permeate concentrations after RO reconcentration, and draw solute rejection by RO. Experiments were performed with an SW30 RO membrane.

Table 5. Draw solute contributed by reverse salt flux (J_s/J_w), corresponding carbon source contributed by J_s/J_w, and carbon source necessary for complete theoretical denitrification to occur for the draw solutions tested. An influent NH_4^+-N concentration of 25 mg/L was used.

Table 6. Draw solution replenishment cost during operation. FO cost is the product of the specific reverse salt diffusion (J_s/J_w) and the draw solution unit cost ($/kg), and RO cost is the product of the RO permeate concentration and the draw solution unit cost. Total cost is the sum of the FO cost and the RO cost.

LIST OF FIGURES

Figure 1. Schematic of an OMBR system. Figure adapted from Ref. [2].

Figure 2. Schematic of an OMBR process salt mass balance.

Figure 3. Flow diagram for draw solution selection for osmotic membrane bioreactor. Figure adapted from Ref. [5].

Figure 4. Schematic of bench-scale FO system. Figure adapted from Ref. [5].

Figure 5. Conductivity-concentration relationship for each draw solution at concentrations corresponding to osmotic pressures of 1.4 MPa, 2.8 MPa, and 4.2 MPa.

Figure 6. Schematic of laboratory-scale MBR system. Samples were collected from this system for batch experiments.

Figure 7. Batch experiment setup to determine effects of selected draw solute on biological performance. Six flasks were bubbled with N_2 to simulate anoxic conditions, and six flasks were bubbled with air to simulate aerobic conditions.

Figure 8. Comparison of reverse salt diffusion (J_s/J_w) for all the organic salts at each osmotic pressure tested with sodium chloride and magnesium chloride results from Ref. [5].

Figure 9. Concentration of a) NO_3^--N and b) TOC as a function of time in an anoxic environment batch experiment. Samples were taken from a membrane bioreactor and spiked with 133 mg/L of sodium propionate (SP), equivalent to 50 mg-C/L, are compared to membrane bioreactor control samples.

Figure 10. Concentration of a) NO_3^--N and b) TOC as a function of time in an aerobic environment batch experiment, Samples taken from a membrane bioreactor and spiked with 133 mg/L of sodium propionate (SP), equivalent to 50 mg-C/L, are compared to membrane bioreactor control samples.

1. INTRODUCTION

Forward osmosis (FO), or engineered osmosis, is the transport of water across a selectively permeable membrane from a solution of higher water chemical potential (lower osmotic pressure) to a solution of lower water chemical potential (higher osmotic pressure). The osmotic pressure difference between the feed solution (lower osmotic pressure) and the draw solution (higher osmotic pressure) serves as a natural driving force for water transport across the membrane [1]. An osmotic membrane bioreactor (OMBR) is a novel type of membrane bioreactor (MBR) system that utilizes a submerged FO membrane inside a bioreactor to recover a high-quality product water from wastewater [2]. In an OMBR system (Figure 1), wastewater is fed into a reactor where it undergoes biological degradation. The FO membrane submerged in the bioreactor separates the mixed liquor from a circulating draw solution, which extracts water from the bioreactor. The membrane acts as a barrier to contaminant transport while allowing water to pass. Water transport from the bioreactor results in dilution of the draw solution. The diluted draw solution is sent to a reconcentration process (such as reverse osmosis (RO) or membrane distillation (MD)) that reconcentrates the draw solution and generates a high-quality product water. When compared to the industry standard for high-quality potable reuse applications (bioreactor, clarifier, microfiltration, reverse osmosis, and advanced oxidation), OMBR systems (bioreactor, forward osmosis, and draw solution reconcentration) have the potential for producing high quality water with fewer processes, reduced footprint, and reduced energy costs [2].

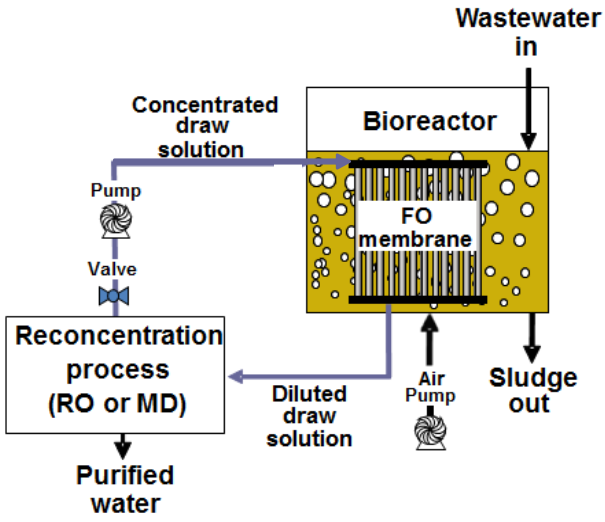

Figure 1. Schematic of an OMBR system. Figure adapted from Ref. [2].

The type of draw solution plays a key role in the OMBR process, affecting FO and bioreactor performance and RO or MD reconcentration; for this reason, selection of an optimal draw solution is an important consideration in the OMBR – or any other FO – system. The osmotic pressure of a specific draw solution depends on the draw solution's characteristics, including molecular size and charge; selection of a draw solution with charged ions and a low molecular weight is desirable to achieve high osmotic pressure and water flux [3, 4]. Researchers have explored several different types of draw solutions for FO applications. In previous studies [1, 5-8], the most commonly used draw solutions were low molecular weight, inorganic ionic salts (e.g., NaCl and $MgCl_2$). Achilli et al. [5] developed a desktop screening process for selection of inorganic ionic salt solutions for use in FO applications and found $MgCl_2$ to be particularly well-suited for environmental applications. Zou et al. [9] also found $MgCl_2$ to outperform NaCl, the most commonly used draw solution, in FO applications. Ammonium bicarbonate, a thermolytic salt, is

being explored by some researchers due to its potential to achieve high water flux and recovery [3]; in order to control the high reverse salt flux [5] associated with the high water flux, specialized membranes are being developed to use with this particular draw solution [10]. Sugars have been investigated as well, but they are uncharged and achieve much lower osmotic pressures than ionic salt solutions [3]. Recently, magnetic nanoparticles coated with hydrophilic polymers (e.g., polyacrylic acid) have been tested because they induce high osmotic pressures; however, agglomeration is a problem when the nanoparticles are magnetically separated for reuse [4]. Two organic draw solutions, polyelectrolytes and 2-methylimidazole-based solutes, have also been studied recently [11, 12]. These studies highlighted benefits that organic draw solutions can offer, such as variable-sized molecules that can be manipulated to achieve desired performance. For example, substituting methyl-groups in a carbon ring to achieve larger molecules creates a draw solute expected to have lower reverse salt flux and lower acidity than in the original five-member ring case while maintaining the properties that make them desirable for use in FO applications.

When considering FO draw solutions for application in an OMBR process, an additional consideration must be addressed: the effects of reverse salt flux on bioreactor performance. Reverse salt flux, or passage of small amounts of draw solute from the draw solution into the feed solution, occurs in all osmotically driven processes because the membranes do not achieve 100 percent rejection [13]. Reverse salt flux negatively affects FO performance efficiency, as it reduces the driving force and necessitates salt replenishment in all FO applications [5]; however, when the feed solution resides in a

bioreactor, additional effects must be considered. These effects include elevated solute concentration in the sludge to be wasted and elevated solute concentration in the bioreactor that may inhibit microbial activity [14-16].

All published OMBR evaluation studies to date (i.e., [2, 14, 15, 17-21]) have only used inorganic salt draw solutions. It has been shown that elevated solute concentrations in the bioreactor do not significantly affect the biological system due to the relatively low concentration reached at steady state [22]. However, it has also been shown that accumulation of inorganic draw solutions will affect OMBR membrane operation and sludge wasting frequency [15].

In the current study, the use of organic ionic salt solutions in OMBR applications is explored. An organic salt is defined as any organic acid (anion) combined with any organic or inorganic base (cation). Rather than accumulating in the bioreactor, the organic anions (and if present, cations) that make up an organic salt draw solution may be biologically degraded. Thus, even though reverse salt flux will still occur, organic draw solutions are not expected to have the accumulation issues that inorganic draw solutions have.

A selection of organic ionic salts was chosen for consideration in this study based on two factors. The first was that increased size adversely affects both achievable osmotic pressure and degree of biodegradability; thus, the smallest anionic organic carbon molecules were selected beginning with a single carbon (formate) and continuing with acetate, propionate, and fumarate/maleate. The second factor in the selection process was choosing salts that could be compared directly with the inorganic salts that have been tested in the literature. Thus, sodium (Na^{+}) and magnesium (Mg^{2+}) were selected as the

cations because experimental results with NaCl and $MgCl_2$ draw solutions are easily available for comparison. The combination of these two cations with the organic anions resulted in a list of ten possible organic ionic salt draw solutions: magnesium formate, magnesium acetate, magnesium propionate, magnesium fumarate, magnesium maleate, sodium formate, sodium acetate, sodium propionate, sodium fumarate, and sodium maleate.

If there is sufficient organic carbon in the influent wastewater for denitrification, the added organic carbon from an ideal draw solution should have biodegradation potential to avoid accumulation in the bioreactor. Denitrification, the final step in total nitrogen removal, may require the addition of an external carbon source to act as an electron donor (e.g., methanol) to be effectively carried out. Shen et al. [23] showed that the addition of an external carbon source was necessary to provide a suitable carbon-to-nitrogen (C/N) molar ratio for complete anoxic denitrification in an MBR system with a nitrate-rich wastewater. Volatile fatty acids, including formate, acetate, propionate, and fumarate, have been found to be effective carbon sources for denitrification [24]. Therefore, if influent wastewater has a C/N ratio that is too low for complete denitrification, reverse salt flux of organic ionic salt draw solutions may provide an additional carbon source for denitrification so that supplemental carbon addition to the bioreactor can be reduced or avoided completely. Furthermore, in an aerobic environment, the volatile fatty acids can provide an additional carbon source in the bioreactor that may allow for denitrificiation to occur even in the presence of oxygen if the C/N ratio is high enough [25].

The objective of this investigation was to evaluate a selection of organic ionic salts as potential draw solutes for an OMBR system. The ideal draw solution would maximize water flux, minimize reverse salt flux, have biodegradation potential and beneficial effects on biological performance, and have reasonable capital and replenishment costs. Results for the organic draw solutes were compared to those for leading inorganic solutes (in terms of performance and cost). In addition to evaluating the organic ionic salts as draw solutions, another goal of this study was to describe a method to determine the diffusion coefficient (D) of a salt solution using a characterized FO membrane. The method presented allows for a fast determination of D for salts whose D values are not directly available in the literature, a capability pertinent to many other engineering applications.

2. THEORY

When considering a draw solution for use in an OMBR system, salt accumulation in the bioreactor must also be considered. Salt loading is introduced to the bioreactor by both the dissolved salts in the influent wastewater and the reverse salt flux into the bioreactor. The salt mass balance in an OMBR system (Figure 2) at equilibrium is:

$$M_{inf} + M_{rsf} = M_{out} + M_{w} \quad (1)$$

where M_{inf} represents the mass of salt entering the bioreactor as influent, M_{rsf} represents the mass entering the bioreactor by reverse salt flux, M_{out} represents the mass of salt that exits the bioreactor in the water that passes through the FO membrane, and M_w represents the mass of salt wasted from the bioreactor. M_{rsf} can be expressed as the specific reverse

salt flux times the permeate volume (V_{out}). M_{out} is assumed equal to zero because salt is almost completely rejected by the FO membrane. Specific reverse salt flux is defined as the ratio between reverse salt flux (J_s) and water flux (J_w), where J_s is the mass of draw solute per area per time time transported from the draw solution into the feed solution and J_w is the volume per area per time of water that is extracted across the membrane by the draw solution [26]. Specific reverse salt flux (J_s/J_w) provides an indication of how much salt is lost during the FO process per each unit volume of water recovered [13]. A low specific salt flux indicates high membrane selectivity and high process efficiency [5].

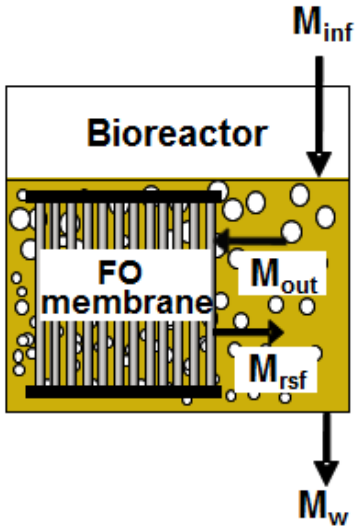

Figure 2. Schematic of an OMBR process salt mass balance.

The terms in Eq. (1) can be expressed using concentration, volume, and specific salt flux as follows:

$$V_{in\,f} C_{in\,f} + V_{out} \frac{J_s}{J_w} = V_w C_b \qquad (2)$$

where V_{inf} is the volume of influent wastewater, C_{inf} is the concentration of salt in the influent wastewater, V_w is the wasted volume of water, and C_b is the concentration of salt in the bioreactor at equilibrium. Knowing that $V_{inf} = V_b/HRT$, $V_w = V_b/SRT$, $V_{out} = V_{inf} - V_w$, and assuming V_b =1 L, Eq. (2) can be rearranged to solve for C_b.

$$C_b = \frac{\frac{1}{HRT} C_{inf} + \left(\frac{1}{HRT} - \frac{1}{SRT} \right) \frac{J_s}{J_w}}{\frac{1}{SRT}} \quad (3)$$

where *HRT* is hydraulic retention time in the bioreactor and *SRT* is sludge retention time in the bioreactor. If the SRT is much greater than the HRT so that 1/HRT-1/SRT ≈ 1/HRT, Eq. (3) can be simplified to:

$$C_b = \left(C_{inf} + \frac{J_s}{J_w} \right) \frac{SRT}{HRT} \quad (4)$$

From Eq. (4), it can be seen that a short HRT coupled with a long SRT (a large SRT/HRT ratio) promotes high salt concentration in an OMBR system [14]. However, Eq. (4) expresses the bulk salt concentration assuming none of the draw solute will biodegrade in the bioreactor. A lower bulk salt concentration as well as improved treatment may be achieved with organic salt draw solutions due to their potential to biodegrade aerobically and aid in denitrification. Ersu et al. [27] reported total nitrogen removal efficiencies for varying MBR systems up to approximately 90 percent with SRTs ranging from 5 to 400 days; typical MBR operation SRTs are between 5 and 25 days [28]. In terms of HRT, MBRs have been successfully operated at HRTs ranging from a few hours to several days [29]. Thus, the most suitable operational parameters can be selected from the typical

ranges to ensure an adequate SRT and HRT for optimal biological treatment while minimizing salt accumulation.

Another consideration when analyzing potential draw solutions is the phenomenon of concentration polarization. Concentration polarization is the concentration or dilution of solutes near an interface, which can severely reduce the effective osmotic pressure difference across the membrane. As a result of water and solute transport across the membrane, solutes are concentrated on the feed-solution side and diluted on the draw-solution side of the membrane surface [30, 31]. Because the membranes used for osmotic processes are typically asymmetric (dense layer on top of a porous support layer), concentration polarization in FO applications occurs externally to the dense layer (feed-solution side) and internally in the support layer (draw-solution side). Concentrative external concentration polarization (ECP), or solute concentration on the feed-solution side of the membrane, causes the osmotic pressure at the membrane surface to be more than the bulk osmotic pressure ($\pi_{F,b}$). However, when the feed solution in FO is pure water ($\pi_{F,b}= 0$), which is the condition for all experiments in this study, ECP does not occur [1, 30].

Dilutive internal concentration polarization (ICP), or solute dilution inside the support layer of the membrane, causes reduced osmotic pressure compared to the bulk solution. To account for ICP effects, the expression for J_w (in units of meters per second) is modified to [30]:

$$J_w = A\left(\pi_{D,b} \exp\left(-J_w K\right)\right) \quad (5)$$

where K is the solute resistivity for diffusion through the thick support layer. The exponent in Eq. (5) is the dilutive ICP modulus ($\pi_{D,i}/\pi_{D,b}$):

$$\frac{\pi_{D,i}}{\pi_{D,b}} = \exp\left(-J_w K\right) \quad (6)$$

where $\pi_{D,i}$ is the osmotic pressure at the dense layer-support layer interface (effective draw solution osmotic pressure) [30]. *K* is calculated using [10]:

$$K = \frac{S}{D} \quad (7)$$

where *S* is the membrane structural parameter and *D* is the solute diffusion coefficient. Eq. (6) can be substituted into Eq. (5) to express the experimental water flux, which accounts for ICP effects, in terms of the water permeability coefficient and the effective draw solution osmotic pressure:

$$J_w = A \cdot \pi_{D,i} \quad (8)$$

Eq. (7) can also be used to calculate *D* by performing FO experiments using a characterized FO membrane with a known *S*. Calculating diffusion characteristics is important in countless engineering applications as it provides information on concentration versus position and time of a desired parameter of interest. Engineered systems involving seawater often require diffusion characteristics when quantifying association and hydration interactions between the seawater and surrounding molecules [32]. Diffusion coefficients are useful in determining mass transport between sediments and seawater or mitigating contamination of fresh groundwater by various seawater sources [32, 33]. In FO applications where solute transport near a membrane surface determines effective driving force, the diffusion coefficient offers insight into effective salt concentrations influencing the driving force of the system. Therefore, determining

the diffusion coefficient is necessary for evaluating a draw solution. Several methods exist for determining diffusion coefficients, but many are complex and have associated uncertainty. Many modern techniques offer more accurate predictions using electrochemical procedures [34], but access to the electrical equipment necessary to perform these experiments is required. The method presented in this study requires only a characterized membrane and FO experiments to determine diffusion coefficient values for the desired ionic salts.

3. MATERIALS AND METHODS

Ten organic salt draw solutions were considered for the OMBR. These salts were analyzed using a modification of the flow diagram for draw solution selection that was developed by Achilli et al. [5]. The diagram was modified to specifically select draw solutions for OMBR systems by adding two criteria (Figure 3). The biodegradability of the organic anion of the draw solution became the first criterion in the selection process and was also included as a laboratory analysis parameter, the goal being to select organic anions that would easily degrade aerobically and/or could act as organic carbon sources that may be required for complete denitrification of nitrate (NO_3^-) in the bioreactor. The other criterion was the commercial availability of the organic ionic salt in the form needed for testing and also the availability of its corresponding technical data (e.g., solubility, hazard, concentration/osmotic pressure relationship, and cost) necessary for desktop screening.

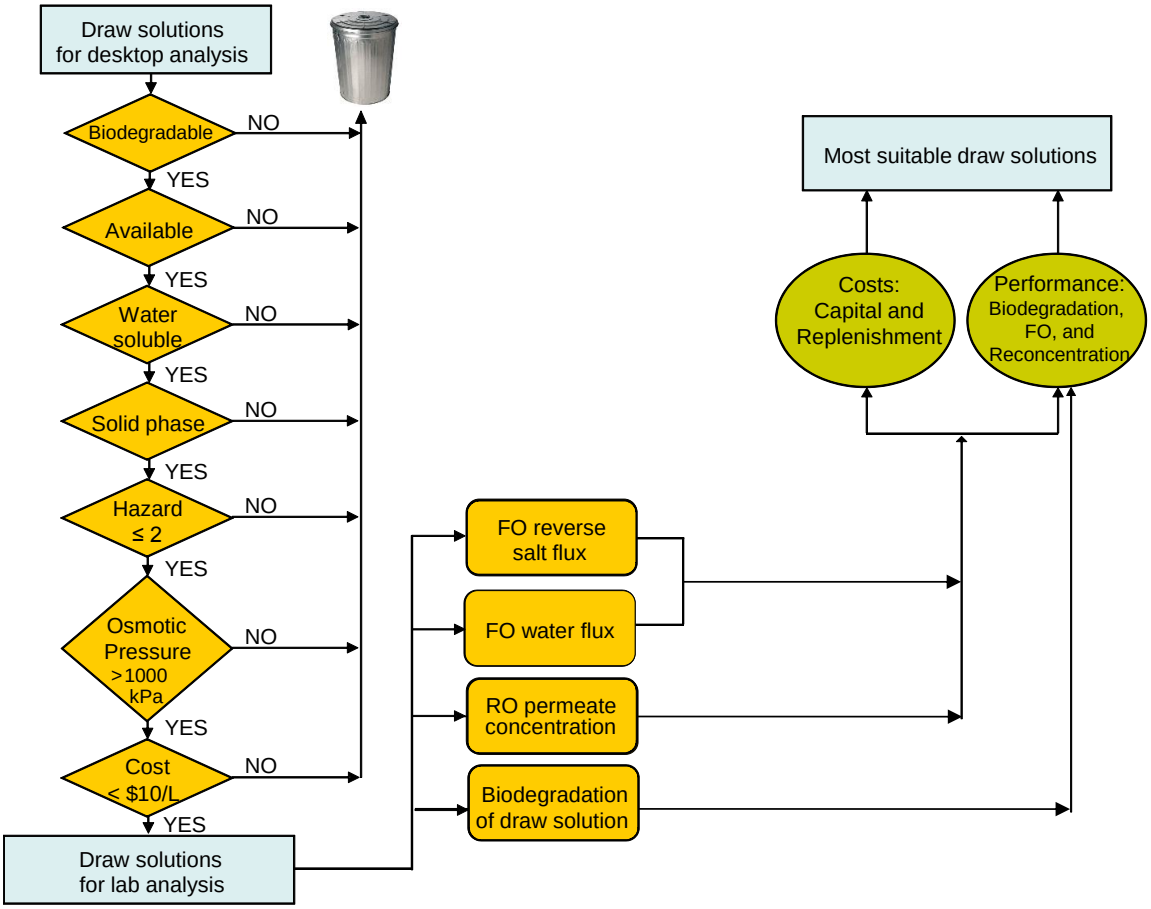

Figure 3. Flow diagram for draw solution selection for osmotic membrane bioreactor. Figure adapted from Ref. [5].

3.1 Desktop Screening Process

Desktop screening was the first step in the draw solution selection process. The first criterion in the screening process, biodegradability, led to the selection of formate, acetate, propionate, and fumarate/maleate as the anions. Fumarate and maleate were soon eliminated because they are not commercially available and must be created in the laboratory with fumaric and maleic acids. Corresponding concentration/osmotic pressure relationships were also unavailable for these acids. The remaining salts were analyzed for

solubility and phase, and all eight were found to be soluble and available in solid form as a salt at ambient temperature and pressure. The Hazardous Materials Identification System (HMIS) codes were then examined to ensure that the health, flammability, and physical hazards of the chemicals were at a level of 2 (moderate hazard) or lower; none of the eight salts were eliminated. Next, OLI Stream Analyzer™ (OLI Systems, Inc., Morris Plains, NJ) was used to obtain the osmotic pressures of the draw solution candidates and to ensure that each had an osmotic pressure of at least 1 MPa (145 psi) at saturation concentration; magnesium propionate did not meet this criterion and was removed from the list. Last, procurement costs of the draw solutes were determined using VWR International unit prices (VWR International, Radnor, PA). Although unit costs are not universal and can vary by region and scale of application, the relative costs of the draw solutes have been found to be fairly constant from supplier to supplier. For this reason, the draw solution selection process focuses on relative rather than absolute costs. Although absolute cost is an important consideration, a draw solution with a slightly higher unit cost should not be disregarded if the other desktop criteria are indicative of a draw solution that warrants further consideration. The specific cost of each draw solution was determined by calculating the cost of solute needed to produce 1 L of draw solution with an osmotic pressure of 2.8 MPa (approximately seawater osmotic pressure). Solutions with a specific cost greater than $10/L were eliminated; magnesium formate had a specific cost of $147/L and was eliminated. The unit costs and osmotic pressures at saturation concentration of the four organic compounds remaining after the desktop screening process are given in Table 1.

Table 1. Draw solution unit costs, specific costs, and osmotic pressures achieved at saturation concentration.

Draw Solution	Draw Solute Unit Cost[+] $/kg	Draw Solution Specific Cost[++] $/L	Osmotic Pressure at Saturation[+++] MPa
Magnesium acetate	41	6.74	10.3
Sodium formate	95	4.36	31.4
Sodium acetate	37	3.38	27.0
Sodium propionate	52	3.41	N.A.*

[+]Unit cost was acquired from VWR International.
[++]Specific cost is the cost to produce 1 L of draw solution with an osmotic pressure of 2.8 MPa.
[+++]Osmotic pressure at saturation was calculated using OLI Stream Analyzer™.
*Value not available in literature

3.2 FO Experiments

3.2.1 Membranes

FO experiments were performed using a flat-sheet cellulose triacetate (CTA) membrane (Hydration Technology Innovations, LLC, Albany, OR). Use of this membrane enabled the collected data to be compared with studies in the literature. The CTA membrane is approximately 50 μm thick with a polyester support mesh between two layers of CTA polymers [3]. The water permeability coefficient (A) of the membrane is 1.87 x 10^{-9} m/s-kPa and the structural parameter (S) of the membrane is 4.27 x 10^{-4} m [5]. The dense layer of the membrane was placed facing the feed solution in all experiments.

3.2.2 Solution chemistries

The draw solutions were prepared by dissolving certified ACS-grade salts (VWR International, Radnor, PA and Fisher Scientific, Pittsburg, PA) in deionized water to achieve the desired concentrations and osmotic pressures. Each draw solution was tested

at three different concentrations to achieve three target osmotic pressures: 1.4, 2.8, and 4.2 MPa (203, 406, and 609 psi).

3.2.3 Laboratory testing apparatus

A schematic of the bench-scale FO system is shown in Figure 4. The modified SEPA-CF membrane test cell (GE Osmonics, Minnetonka, MN) had both feed-side and draw-side channels for tangential flow. Each channel was 14.5 cm long, 11.5 cm wide, and 0.25 cm deep with an effective membrane area of 139 cm^2. Mesh spacers were added on either side of the membrane for additional support. The draw solution circuit was connected to a re-circulating chiller (Fisher Scientific, Pittsburg, PA) to maintain the solution temperature at a constant 25 ^oC. Two variable-speed gear pumps (Cole-Parmer, Vernon Hills, IL) re-circulated the feed and draw solutions at a rate of 1.5 L/min on each side of the membrane. Deionized water was used as the feed solution for all experiments. The feed solution reservoir was held at a constant volume of 5.4 L by a second reservoir of deionized water that continuously replenished the feed solution reservoir as water was transported across the membrane. The second deionized water reservoir was placed on an analytical balance connected to a computer to record volume lost. Water flux (J_w), in units of liters per square meter hour (LMH), was quantified by measuring the water lost from the deionized water reservoir divided by a set time period between readings (Δt) and the effective membrane area (A_m):

$$J_w = \frac{(m_{t2} - m_{t1})}{\Delta t \cdot A_m \cdot \rho_w} \qquad (9)$$

where m_{t1} and m_{t2} are the recorded masses at times t_1 and t_2, and ρ_w is the density of water.

The concentration of salt in the feed solution (C_f) was monitored to quantify reverse salt flux (J_s), in units of grams per square meter per hour. A conductivity probe (Accumet Basic, Fisher Scientific, Hampton, NH) was used to determine the change in conductivity in the feed solution. This was converted to a change in concentration using a linear relationship developed from OLI Stream Analyzer. The concentration was then multiplied by the volume of the feed solution reservoir (V_f) and divided by a set time period between readings (Δt) and the effective membrane area (A_m):

$$J_s = \frac{\left(C_{f,t2} - C_{f,t1}\right) \cdot V_f}{\Delta t \cdot A_m} \tag{10}$$

where $C_{f,t1}$ and $C_{f,t2}$ are the calculated concentrations of the feed at times t_1 and t_2.

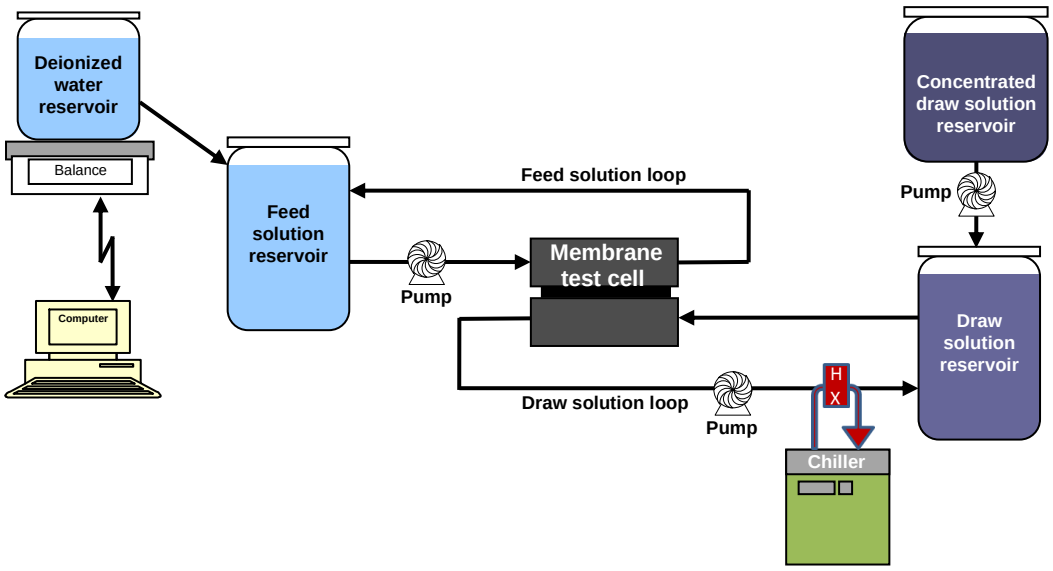

Figure 4. Schematic of bench-scale FO system. Figure adapted from Ref. [5].

The 10-L draw solution reservoir was held at a constant salt concentration by a second reservoir of highly concentrated draw solution that fed fixed amounts of the draw

solution. When the concentration in the draw solution reservoir dropped below the initial conductivity (due to water flux from the feed solution reservoir diluting the draw solution), draw solution was dosed from the concentrated draw solution reservoir until the original draw solution concentration was restored. Draw solution concentration was monitored using a conductivity probe (Accumet Basic, Fisher Scientific, Hampton, NH).

3.2.4 FO testing procedure

Prior to each experiment, the bench-scale FO system was flushed with deionized water for 30 min and the feed reservoir was filled with deionized water. The initial conductivity of the solution was recorded with the same conductivity probe that was submerged in the draw solution reservoir for the duration of the experiment to monitor concentration (using conductivity-concentration relationships). The conductivity probe readings were automatically recorded every second to ensure that a constant draw solution concentration was maintained in the reservoir.

Throughout the experiments, conductivity was used as a surrogate measure for solute concentration because typically, the conductivity of a solution is proportional to its ion concentration. This was true at the osmotic pressures tested for sodium formate, sodium acetate, sodium propionate, and the lower concentrations of magnesium acetate (osmotic pressures of 1.4 and 2.8 MPa). In the case of the highest concentration of magnesium acetate (osmotic pressure of 4.2 MPa), however, this was not the trend. Conductivity decreased slightly at the highest osmotic pressure of magnesium acetate. In some salts, ionic interactions can make the electrons less available and reduce electrical current flow, thus reducing the conductivity readings at higher concentrations [35]. This phenomenon did not affect the other salts that were tested because they reached

saturation concentration before ionic interactions became an issue, maintaining an approximately linear conductivity-concentration relationship (Figure 5). The three points used to construct the conductivity-concentration relationship for each salt represent the three osmotic pressures (1.4 MPa, 2.8 MPa, 4.2 MPa) that the FO experiments were run. Because magnesium acetate requires relatively high salt concentrations to achieve an osmotic pressure of 4.2 MPa, but still remains below saturation concentration, it is likely that ionic interactions affect the linear relationship. This discovery is significant because it prohibited use of the method of dosing a high concentration solution to the draw solution reservoir and limited the experimental data taken for the 4.2 MPa magnesium acetate draw solution to the first few hours of testing when the driving force remained constant and did not begin to decline due to dilution. Therefore, ionic interactions and the corresponding effects on the conductivity readings within a desired operating range must be considered with any future draw solute selections.

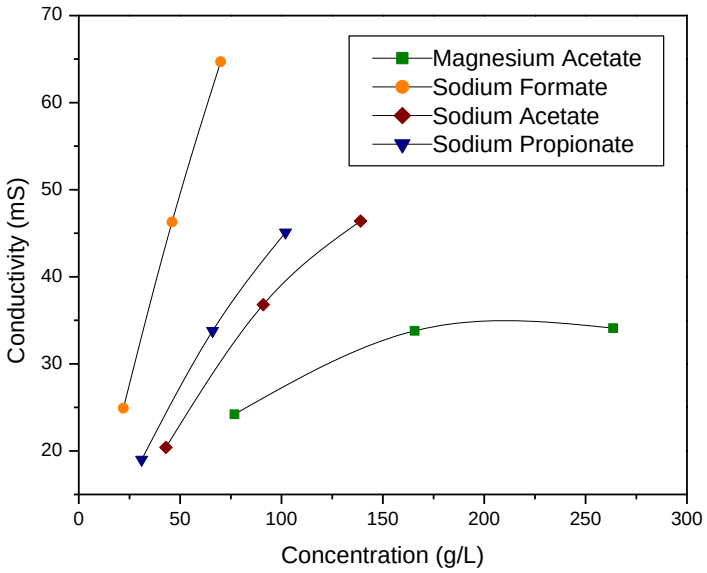

Figure 5. Conductivity-concentration relationship for each draw solution at concentrations corresponding to osmotic pressures of 1.4 MPa, 2.8 MPa, and 4.2 MPa.

Each experiment was run for a minimum of six hours. Water flux, conductivity in the feed and draw solution reservoirs, and pH in the feed and draw solution reservoirs were measured. Experiments were run twice at each osmotic pressure and results were averaged. Following the FO experiments, the diffusion coefficient for each solution was calculated by rearranging Eq. (7) to solve for *D*. *S* is a constant value dependent on membrane characteristics and was taken to be 4.27×10^{-4} m from previous experiments using the same CTA membrane [5]. *K* was determined using Eq. (5).

3.3 RO experiments

3.3.1 Membranes

RO reconcentration experiments were performed using an SW30 polyamide thin-film composite membrane (Dow Filmtec, Midland, MI). The SW30 membrane consists of three layers and was selected due to its capability of operating at up to 6.9 MPa (1,000 psi) while maintaining high water flux and salt rejection.

3.3.2 Solution chemistries

The draw solutions were prepared using certified ACS-grade salts (VWR International, Radnor, PA and Fisher Scientific, Pittsburg, PA) dissolved in deionized water. Salt concentrations corresponding to an osmotic pressure of 1.4 MPa were used for all RO reconcentration experiments.

3.3.3 Laboratory testing apparatus

A bench-scale SEPA-CF membrane test cell (GE Osmonics, Minnetonka, MN) was used for the RO experiments. The test cell was similar to that used for the FO experiments, except it had only a feed-side channel for tangential flow of the feed

solution. Mesh spacers were added on either side of the membrane for additional support. The test cell was connected to a re-circulating chiller (Fisher Scientific, Pittsburg, PA) to maintain the solution temperature at a constant 20 ^{o}C. A positive displacement pump (Wanner Engineering Inc., Minneapolis, MN) was used to re-circulate the feed solution at 1.5 L/min. The feed solution was contained in a 4-L reservoir. The system was run under constant flux conditions.

3.3.4 Testing procedure

RO reconcentration tests were performed using a constant pressure of 2.8 MPa (406 psi). Flux through the membrane was measured by the change in weight over time of the permeate reservoir resting on an analytical balance. The conductivity of the permeate was measured with a conductivity probe (Accumet Basic, Fisher Scientific, Hampton, NH) after approximately 100 g of permeate had been collected; then the permeate was returned to the feed reservoir to maintain a constant feed concentration (C_f). The recorded conductivity was then used to find the solute concentration in the permeate (C_p) and the corresponding rejection, R:

$$R = 1 - \frac{C_P}{C_F} \cdot 100 \qquad (11)$$

3.4 Biodegradation quantification

3.4.1 Prediction of biological performance

Following FO experiments, the biodegradation potential of each organic salt was predicted and quantified. Specific salt flux (J_s/J_w) was used to quantify the amount of salt that would be transported into the bioreactor from the draw solution. Specific salt flux provided an indication of the amount of organic anion available as a potential carbon

source for denitrification in the cases where carbon is the limiting factor. The following nitrification and denitrification reactions were used to determine the amount of solute necessary for complete removal of influent NH_4^+, which first undergoes nitrification where NH_4^+ is oxidized to NO_3^-, and then denitrification where NO_3^- is reduced to N_2 gas:

Nitrification:

$$NH_4^+ + 2O_2 \rightarrow NO_3^- + 2H^+ + H_2O \quad (12)$$

Denitrification:

$$\text{Carbon source} + aNO_3^- + bH^+ \rightarrow cN_2 + dCO_2 + eHCO_3^- + fH_2O \quad (13)$$

where *a-f* are coefficients that vary depending on the carbon source utilized as the electron donor (e.g., formate, acetate, and propionate). An influent NH_4^+-N of 25 mg/L was used, assuming a medium-strength wastewater influent [28]. The amount of solute necessary for denitrification was then compared to the amount of solute transported into the bioreactor by reverse salt flux.

3.4.2 Batch biological experiments

Batch experiments were designed to evaluate the biodegradation of the organic salt that would enter the bioreactor through reverse salt flux and to evaluate the effect of the organic salt on biological performance. Samples for the batch experiments were collected from a laboratory-scale MBR system, operating with separate anoxic and aerobic reactors (Figure 6) to achieve combined nitrification/denitrification and organic carbon removal. Influent synthetic wastewater containing glucose and peptone representing medium-strength domestic wastewater [28], was pumped directly into the anoxic reactor, where hydraulic mixing occurred at a rate of 250 rpm. An effluent line (at

the water surface of the anoxic reactor) allowed for gravity flow from the anoxic reactor into the aerobic reactor. A recycle line situated one inch from the bottom of the aerobic reactor recycled mixed liquor back into the anoxic reactor via a peristaltic pump. A membrane cassette (Kubota Membrane Corp., USA) was submerged in the aerobic reactor. The cassette contained a microfiltration membrane having a nominal pore size of 0.22 µm to achieve solids separation. An effluent line connected to the membrane cassette was pumped at the same flow rate to achieve an HRT of 2 days. An SRT of 30 days was maintained by wasting mixed liquor from the aerobic reactor. A perforated plastic pipe along the bottom of the aerobic reactor was used to disperse air flow evenly and continuously at a rate of 1 L/min.

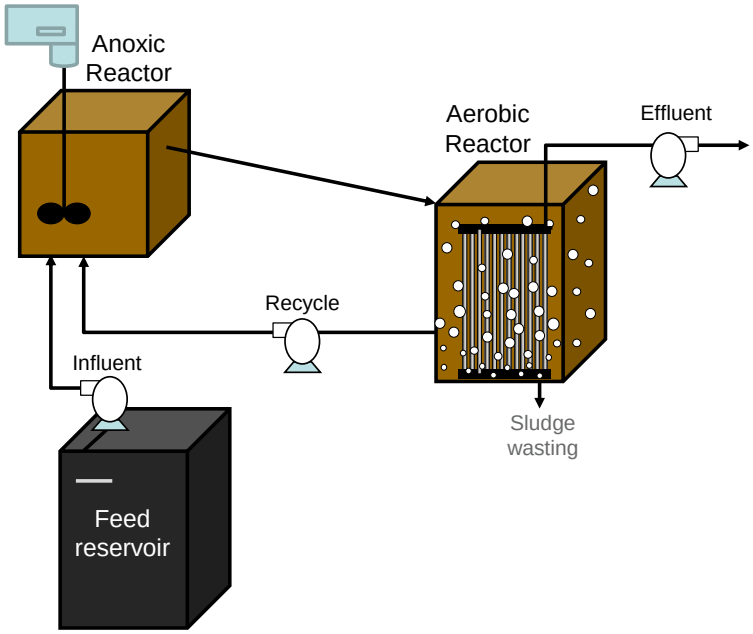

Figure 6. Schematic of laboratory-scale MBR system. Samples were collected from this system for batch experiments.

A 2.4-L sample was taken from the aerobic reactor of the MBR to determine whether the organic carbon contributed by the draw solute would readily degrade during aerobic periods in the bioreactor. These samples were collected and diluted with 0.6 L of distilled water, separated equally into six identical 2-L flasks (for a total of 500 mL of sample in each flask), and aerated continuously with air to simulate aerobic conditions in an OMBR. Also of interest was whether the added organic carbon would promote denitrification in an aerobic environment. Draw solute was added to three of the samples while the other three flasks were unaltered to act as controls. Samples were analyzed for NO_3^--N (using a Lachat QuikChem 8500 Automated Ion Analyzer, Lachat Instruments, Loveland, CO) and TOC (using a Shimadzu Total Organic Carbon Analyzer, Shimadzu Scientific Instruments, Kyoto, Japan)).

In order to determine the effect of the additional carbon source provided by reverse transport of the draw solute on denitrification in the bioreactor, a 2.4-L sample was taken from the anoxic reactor of the MBR, diluted with 0.6 L of distilled water, separated equally into six identical 2-L flasks (for a total of 500 mL of sample in each flask), and deaerated continuously with N_2 gas to simulate anoxic conditions in an OMBR (Figure 7). The same amount of draw solute was added to three samples while the other three were unaltered to act as controls. Since the sample was taken from a working anoxic reactor, the initial concentrations of NO_3^--N was approximately zero, so all six samples were spiked with 20 mg/L NO_3^--N (using $NaNO_3$) to obtain a large enough initial concentration of NO_3^- to observe degradation over a period of several hours. Samples were analyzed for NO_3^-- N and TOC every 45 min until NO_3^- was completely

degraded to determine the relative rates at which the NO_3^- would degrade via anoxic dentirification.

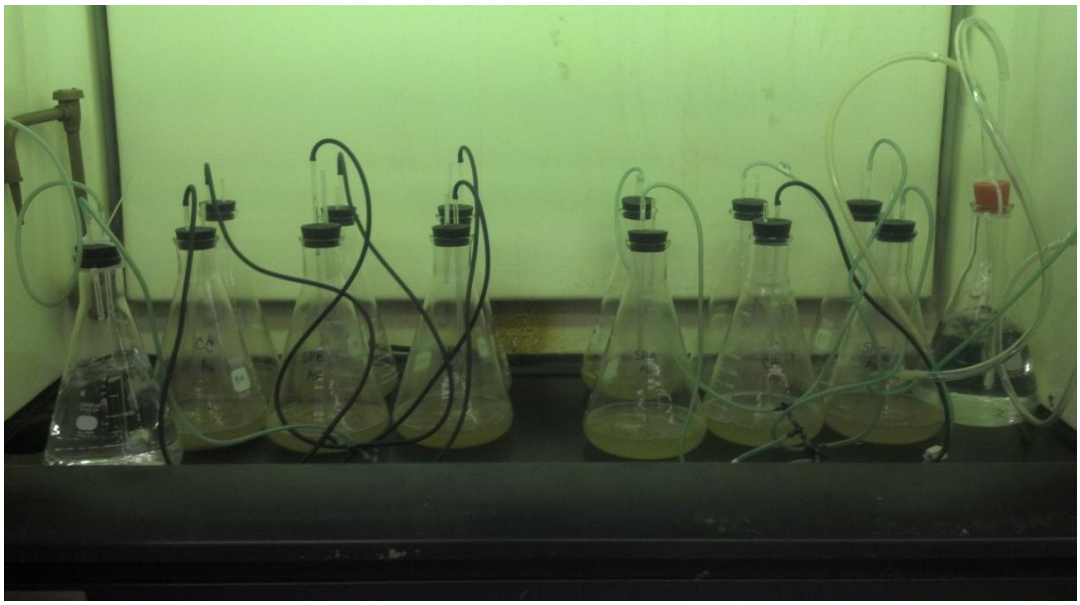

Figure 7. Batch experiment setup to determine effects of draw solute on biological performance. Six flasks were bubbled with N_2 to simulate anoxic conditions (left), and six flasks were bubbled with air to simulate aerobic conditions (right).

3.5 Replenishment cost determination

FO salt loss resulted from the reverse salt flux from the draw solution to the feed solution. FO replenishment costs were determined by multiplying J_s/J_w by the cost per kg of the bulk salt (from Table 1) to achieve a cost per liter. RO salt loss resulted from salt passage through the RO membrane along with the finished product water. RO replenishment costs were determined by multiplying the RO permeate concentration by the cost per kg of the bulk salt. Total replenishment cost was the sum of the FO replenishment cost and the RO replenishment cost.

4. Results and Discussion

4.1 Water flux

The water flux (J_w) data is summarized in Table 2. In all cases, as the osmotic pressure increased, the water flux increased due to the increased driving force. At 2.8 MPa osmotic pressure, water flux values range from 2.60 x 10^{-6} m/s for sodium formate to 2.25 x 10^{-6} m/s for magnesium acetate. The difference between these values is most likely due to internal concentration polarization. Internal concentration polarization, or the dilution of the draw solution in the support layer of the membrane, reduced the effective osmotic pressure difference across the membrane to varying degrees for each salt. A salt with a low diffusion coefficient is less likely to diffuse into the membrane support layer and cause decreased concentration of the draw solution within the support layer and. The reduced draw solute inside the support layer causes more severe internal concentration polarization effects [36]. In the case of the magnesium acetate draw solution, there is a more noticeable difference between the diffusion coefficients at the three different osmotic pressures, with a 0.23 x 10^{-9} m^2/s reduction in D with each increase in osmotic pressure. An increased viscosity of this salt solution was observed at the higher osmotic pressures (not observed in the other salts tested) and may be the reason for the reduction in the diffusion coefficient, as the more viscous magnesium acetate was not as readily able to diffuse into the porous support layer.

Table 2. Aqueous solution osmotic pressure (π_{DS}), concentration (C_{DS}), water flux (J_w), solute resistivity (K), and diffusion coefficient (D) for each draw solution.

Draw Solution	π_{DS} MPa	C_{DS} g/L	J_w 10^{-6} m/s	K 10^5 s/m	D 10^{-9} m^2/s
Sodium formate	1.4	22	1.65	2.82	1.51
	2.8	46	2.60	2.69	1.59
	4.2	70	3.25	2.72	1.57
Sodium acetate	1.4	43	1.61	3.02	1.41
	2.8	91	2.50	2.96	1.44
	4.2	139	2.89	3.47	1.23
Sodium propionate	1.4	31	1.54	3.44	1.24
	2.8	66	2.41	3.22	1.33
	4.2	102	2.97	3.28	1.30
Magnesium acetate	1.4	77	1.59	3.12	1.37
	2.8	166	2.25	3.75	1.14
	4.2	264	2.47	4.70	0.91

The experimentally measured water flux was input into Eq. (5) to determine the solute resistivity (K) for each solution. Then, using Eq. (7) and the constant value of 4.27 x 10^{-4} m for the structural parameter (S) for the CTA membrane, the diffusion coefficient (D) was found for each solution. Values of K and D for each draw solution are given in Table 2. This method of determining D is useful because, unlike D values for inorganic salts, D values for many organic salts are not directly available in the literature and accurate predictions often require electrochemical procedures. Using FO experiments to determine D values only requires knowledge of the structural parameter and determination of K by FO experiments.

4.2 Reverse salt flux

The reverse salt flux (J_s) for each of the organic ionic salt concentrations tested is given in Table 3. When comparing magnesium acetate and sodium acetate, which have

the same anion species, the reverse salt flux of magnesium acetate was less than half that of sodium acetate. This observation is supported by the literature, which indicates that the larger cations result in decreased salt flux across the membrane [5]. There is a similar trend with the size of the organic carbon anion; when comparing the sodium salts containing between one and three carbons, from propionate (C_3) to acetate (C_2) to formate (C_1), the reverse salt flux increases.

Table 3. Aqueous solution osmotic pressure (π_{DS}), concentration (C_{DS}), reverse salt flux (J_s), water flux (J_w), effective osmotic pressure ($\pi_{D,i}$), effective draw solution concentration ($C_{D,i}$), and specific reverse salt flux (J_s/J_w). $\pi_{D,i}$ was calculated using Eq. (6) and the corresponding $C_{D,i}$ was calculated using OLI Stream Analyzer™.

Draw Solution	π_{DS} **MPa**	C_{DS} **g/L**	J_s **g/m^2 h**	J_w **10^{-6} m/s**	$\pi_{D,i}$ **MPa**	$C_{D,i}$ **g/L**	J_s/J_w **g/L**
Magnesium acetate	1.4	77	0.63	1.59	0.85	43.4	0.11
	2.8	166	1.07	2.25	1.20	64.5	0.13
	4.2	264	1.06	2.47	1.34	72.7	0.12
Sodium propionate	1.4	31	0.80	1.54	0.82	18.3	0.15
	2.8	66	1.47	2.41	1.29	29.5	0.17
	4.2	102	2.29	2.97	1.59	36.6	0.21
Sodium acetate	1.4	43	1.50	1.61	0.86	26.9	0.26
	2.8	91	2.73	2.50	1.34	42.5	0.30
	4.2	139	3.55	2.89	1.54	49.1	0.34
Sodium formate	1.4	22	3.86	1.65	0.88	13.8	0.65
	2.8	46	6.04	2.60	1.39	22.2	0.65
	4.2	70	7.63	3.25	1.74	28.2	0.65

In all but one case (magnesium acetate), as the osmotic pressure increased, the reverse salt flux increased. The reverse salt flux and water flux of the magnesium acetate leveled off as the osmotic pressure increased from 2.8 MPa to 4.2 MPa. This is likely due to the viscosity of the highly concentrated magnesium acetate solution, which noticeably increased in this range and may have adversely affected the salt's ability to diffuse into

the membrane support layer, thereby causing an increase in internal concentration polarization effects.

4.3 Specific salt flux

The specific salt flux (J_s/J_w) is also included in Table 3. This is a valuable parameter for evaluating draw solution performance because a low J_s/J_w indicates low salt loss with respect to water flux. The values for J_s/J_w remained relatively constant for each salt, which is consistent with previous findings that specific salt flux is independent of concentration [5, 37]. In Figure 8, results for J_s/J_w for the organic draw solutions are compared with those for NaCl and $MgCl_2$, two commonly used inorganic ionic salt draw solutions. The highest performing draw solution with respect to specific salt flux was magnesium acetate with an average J_s/J_w of 0.12 g/L. The specific salt flux for magnesium acetate was 6.2 times lower than that reported for NaCl (approximately 0.74 g/L) using the same bench-scale FO system. In addition, magnesium acetate had a J_s/J_w of over 4.5 times lower than that reported for $MgCl_2$ (approximately 0.58 g/L), which has recently received attention because of its potential for better performance (relative to NaCl) in water treatment applications [5, 9]. The organic draw solution with the highest J_s/J_w was sodium formate with 0.65 g/L; which is still lower than that of sodium chloride.

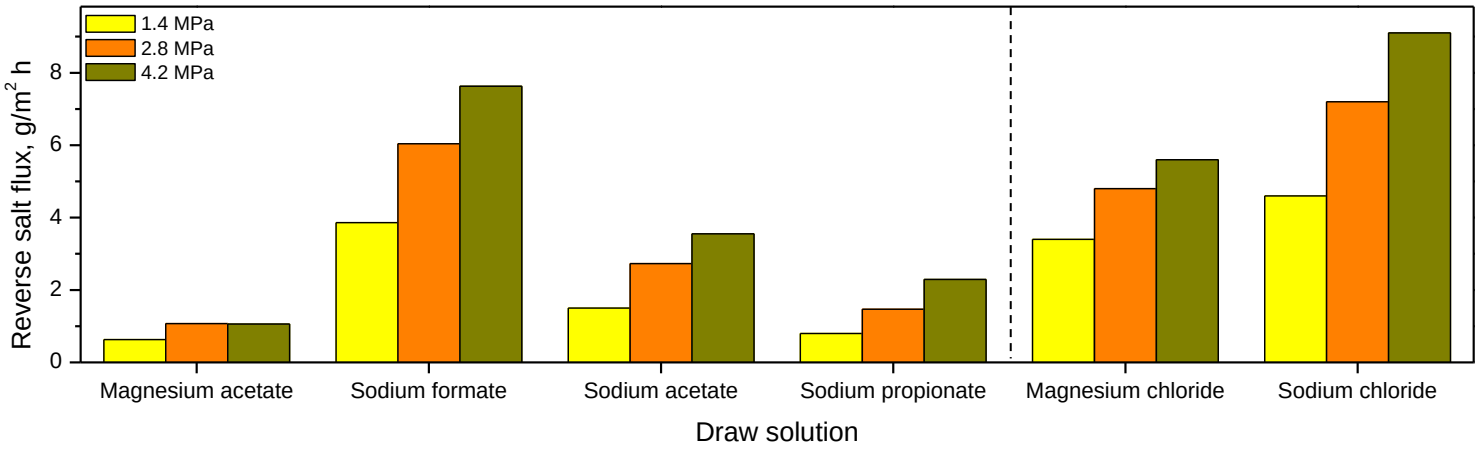

Figure 8. Comparison of reverse salt diffusion (J_s/J_w) for all the organic salts at each osmotic pressure tested with sodium chloride and magnesium chloride results from Ref. [5].

Eq. (4) was used to determine the bulk salt concentration in the bioreactor using calculated specific salt flux values for each salt to determine whether salt accumulation would be a concern. Values expected for a pilot-scale OMBR system currently being implemented in the laboratory were input into the equation, where the salt concentration in the influent (C_{inf}) was 41 mg/L (medium-strength wastewater), the SRT was 30 days, and the HRT was 2 days. Using the specific salt flux of magnesium acetate and sodium propionate (the two highest performing salts expected to be implemented in a future pilot-scale system), bulk salt concentrations were found to be 2.4 g/L and 3.2 g/L, respectively, which are both low enough not to be a concern [16].

4.4 RO Reconcentration

RO experiments were performed to evaluate RO rejection for each of the organic ionic salt solutions. The rejections of NaCl and $MgCl_2$ at the same osmotic pressure were used for comparison. In Table 4, the concentration of each draw solution corresponding to an osmotic pressure of 1.4 MPa, RO permeate concentration (C_p), and rejection (R) are given. The organic ionic salt rejections were high in all cases, near and exceeding 99 percent. With the exception of sodium formate, all of the organic ionic salts had higher rejections than NaCl. This indicates that implementing an RO reconcentration loop for these organic salt draw solutions is feasible for an OMBR system. Regarding the permeate concentration, it was assumed that the paired anions and cations diffuse across the membrane at nearly the same rate in order to maintain electroneutrality. Future work should test this assumption and determine the exact concentration of cation and organic anion in the RO permeate.

Table 4. Draw solution concentrations corresponding to an osmotic pressure of 1.4 MPa, permeate concentrations after RO reconcentration, and draw solute rejection by RO. Experiments were performed with an SW30 RO membrane.

Draw Solution	**C_{DS}**	**C_P**	**R**
	g/L	**mg/L**	**%**
Magnesium acetate	77	589	>99
Sodium formate	22	295	98.7
Sodium acetate	43	185	>99
Sodium propionate	31	192	>99
NaCl	18	190	98.9
$MgCl_2$	33.8	111.5	>99

4.5 Biodegradation of draw solutions

4.5.1 Prediction of biological performance

In Table 5, the amount of carbon source that is theoretically utilized during the denitrification process was compared to the amount of carbon source contributed by the organic draw solute via reverse salt flux. Theoretical values were determined using half reactions for nitrification/denitrification, and the amount of the organic draw solute contributed by reverse salt flux was taken to be the average J_s/J_w value for magnesium acetate (0.12 g/L), sodium formate (0.65 g/L), sodium acetate (0.3 g/L), and sodium propionate (0.18 g/L). These values are proportional to the carbon source available for denitrification if the organic carbon in the original wastewater influent is limiting and the system requires an additional carbon source for denitrification. For sodium propionate, 0.14 g/L of carbon source (propionate) is contributed by reverse salt flux, and 0.05 g/L of carbon source is required for complete denitrification of NO_3^-, so up to one third of the propionate transported into the reactor by reverse salt flux could be utilized for denitrification and not contribute to salt accumulation. These theoretical predictions

suggest that the organic carbon source will be partially used in denitrification; however, there will be a surplus of the organic carbon supply. Biological batch experiments in an aerobic environment were performed to confirm that the organic salt present in the bioreactor would readily degrade if there is a surplus that is not being utilized for denitrification.

Table 5. Draw solute contributed by reverse salt flux (J_s/J_w), corresponding carbon source contributed by J_s/J_w, and carbon source necessary for complete theoretical denitrification to occur for the draw solutions tested. An influent NH_4^+-N concentration of 25 mg/L was used.

Draw Solution	**Draw solute contributed by J_s/J_w**	**Carbon source contributed by J_s/J_w**	**Carbon source necessary for denitrification**
	g/L	**g/L**	**g/L**
Magnesium acetate	0.12	0.10	0.07
Sodium formate	0.65	0.43	0.20
Sodium acetate	0.30	0.22	0.07
Sodium propionate	0.18	0.14	0.05

4.5.2 Batch biological experiments

Sodium propionate was selected as the draw solution to be added to the samples in the batch experiments due to its high performance characteristics during desktop screening and FO and RO experiments. A concentration of 133 mg/L of sodium propionate (equivalent to 100 mg/L of propionate carbon source and 50 mg TOC/L) was added to the samples. This concentration was selected so that the range of TOC concentrations in the samples could be detected by the analysis equipment without

requiring dilution or concentration of the samples that could lead to uncertainty in the results.

Anoxic reactor samples were spiked with 20 mg NO_3^--N/L to determine the relative rates of denitrification of the samples with added sodium propionate (SP samples) and the control samples. The NO_3^--N and TOC concentrations in the anoxic reactor samples were monitored for 4.75 hr (Figure 9). The first sample for the batch experiment was taken 15 min after N_2 sparging began. The data in Figure 9a represent the degradation of NO_3^--N with time, beginning with the initially spiked concentration of 20 mg NO_3^--N/L. The SP samples degraded more than three times faster than the control samples. The SP samples degraded at a rate of 3.6 ± 0.06 mg NO_3^--N/hr, with complete degradation after approximately 4.75 hr. The controls degraded at a rate of 1.0 ± 0.08 mg NO_3^--N/hr, with complete degradation projected after 19 hr (assuming a constant degradation rate). A sample taken at 24 hr confirmed complete degradation of NO_3^--N in both the controls and the SP samples. The presence of readily biodegradable propionate available as an electron donor increased the rate of denitrification more than three times in an anoxic environment, enhancing nitrogen removal.

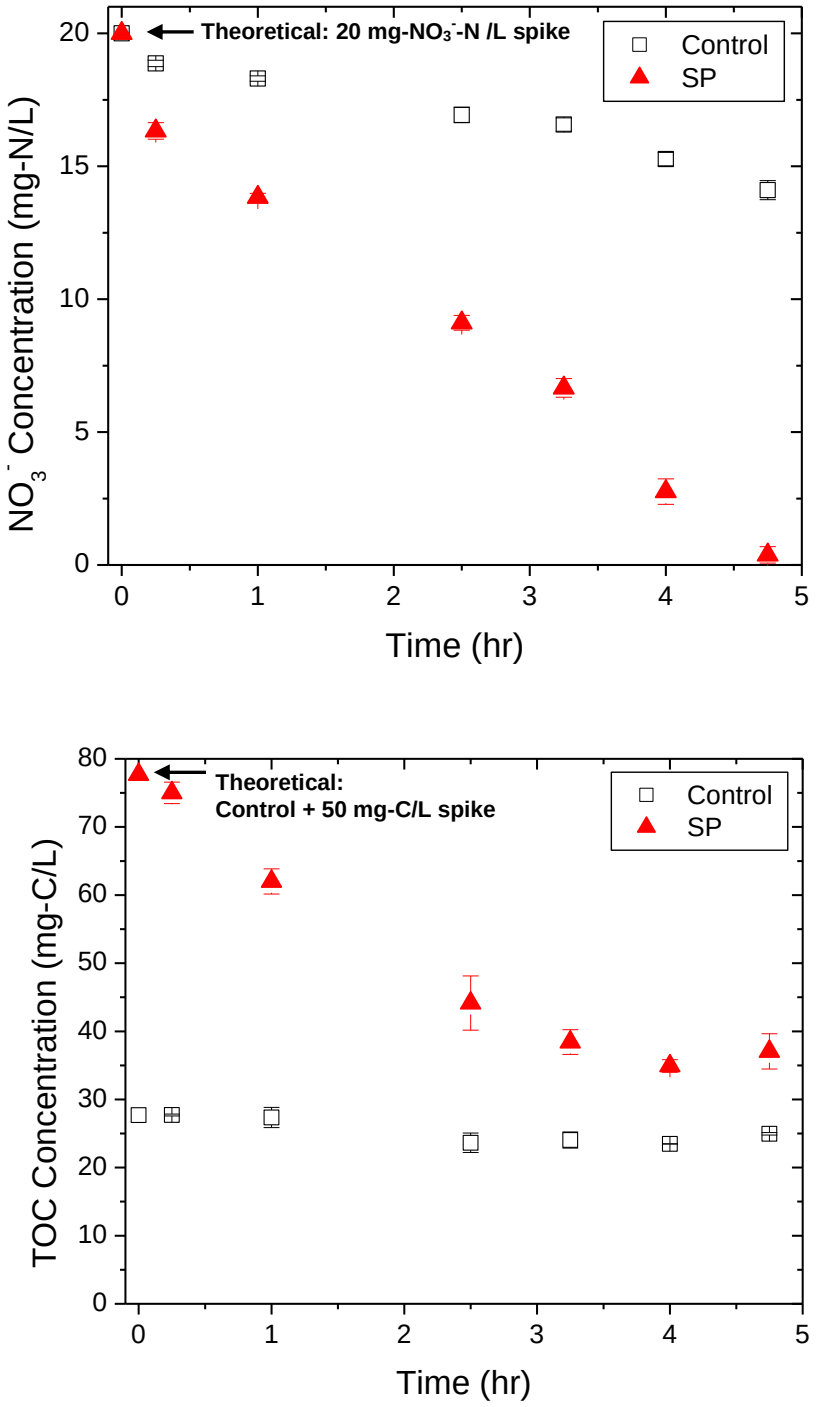

Figure 9. Concentration of a) NO_3^--N and b) TOC as a function of time in an anoxic environment batch experiment. Samples were taken from a membrane bioreactor and spiked with 133 mg/L of sodium propionate (SP), equivalent to 50 mg-C/L, are compared to membrane bioreactor control samples.

The data in Figure 9b represent TOC concentration as a function of time, beginning with the initial average concentrations of 27.7 mg C/L in the control samples and 77.5 mg C/L in the SP samples. The TOC reduction over 4.5 hr in the SP samples was 40.3 mg/L, whereas for the control samples, the drop in TOC was only 2.7 mg/L (due to the slower rate of denitrification, as observed in Figure 9a). TOC concentrations level off in the SP samples, likely due to the lack of NO_3^--N available as an electron acceptor as denitrification approaches completion. Results from this experiment confirm that as predicted, denitrification utilizes propionate. Theoretical half reactions predict that for every mg of NO_3^--N degraded, approximately 1 mg of TOC (assuming propionate is the carbon source) is required. Experimentally, it was found that for every mg of NO_3^--N degraded, 2.1 mg of TOC were degraded, twice the theoretical prediction, which can likely be attributed to carbon also being utilized for various other metabolic activities. Also, the amount of propionate added to the bioreactor is greater than the amount of propionate necessary for complete denitrification of the NO_3^-. When comparing the TOC concentration of the controls with the SP samples at 4.75 hr, the SP samples contain approximately 8 mg C/L more than the control samples, indicating a surplus of organic carbon (as predicted in Section 4.5.1).

The NO_3^--N and TOC concentrations in the aerobic reactor samples were monitored for 4.5 hr (Figure 10) to determine the biodegradation and denitrification potentials of the samples in an aerobic environment. The first sample for the batch experiments was taken 30 min after beginning aerating the flasks. In the 30 min that elapsed between the start of aeration and NO_3^--N/TOC analysis, the concentration of the samples with the added sodium propionate dropped from approximately 4.6 mg NO_3^--

N/L to 2.5 mg NO_3^--N/L. There are two possible explanations for this drop in NO_3^--N concentration. One is that conditions are suitable for partial aerobic denitrification, likely due to the high concentration of readily available organic carbon source (C/N ratio of 3.9). However, it is important to note that the NO_3^--N does not degrade completely in the SP samples, which may be an indication of an initial period of low dissolved oxygen as an alternative explanation for the initial drop in NO_3^--N. While the samples were transitioning into an aerobic environment, denitrification could occur due to the low oxygen environment rather than the high C/N ratio. When comparing the SP samples with the control samples, the control samples experienced an identical environmental shift and no reduction in NO_3^--N, demonstrating that the presence of the sodium propionate does in fact affect the NO_3^--N degradation. In order to investigate this further, an additional batch experiment (data not shown) was conducted with the same experimental setup, but with a sodium propionate spike of 3,000 mg/L and an NO_3^--N concentration in the aerobic MBR of 8.0 mg/L (for a C/N ratio of 140, significantly higher than the previous experiment). The NO_3^--N concentration in the SP samples had dropped to 6.4 mg/L when a sample was taken 1.5 hr after aeration began, while the concentration in the controls remained constant. Complete degradation of NO_3^- was observed in the SP samples after 24 hr, while the NO_3^-- N concentration in the control samples increased slightly. These preliminary results demonstrate the denitrification potential with the high concentration of available organic carbon (high C/N ratio). On the other hand, the slight increase in NO_3^-- N concentration in the control samples indicate that conditions without the added carbon source are not suitable for aerobic denitrification.

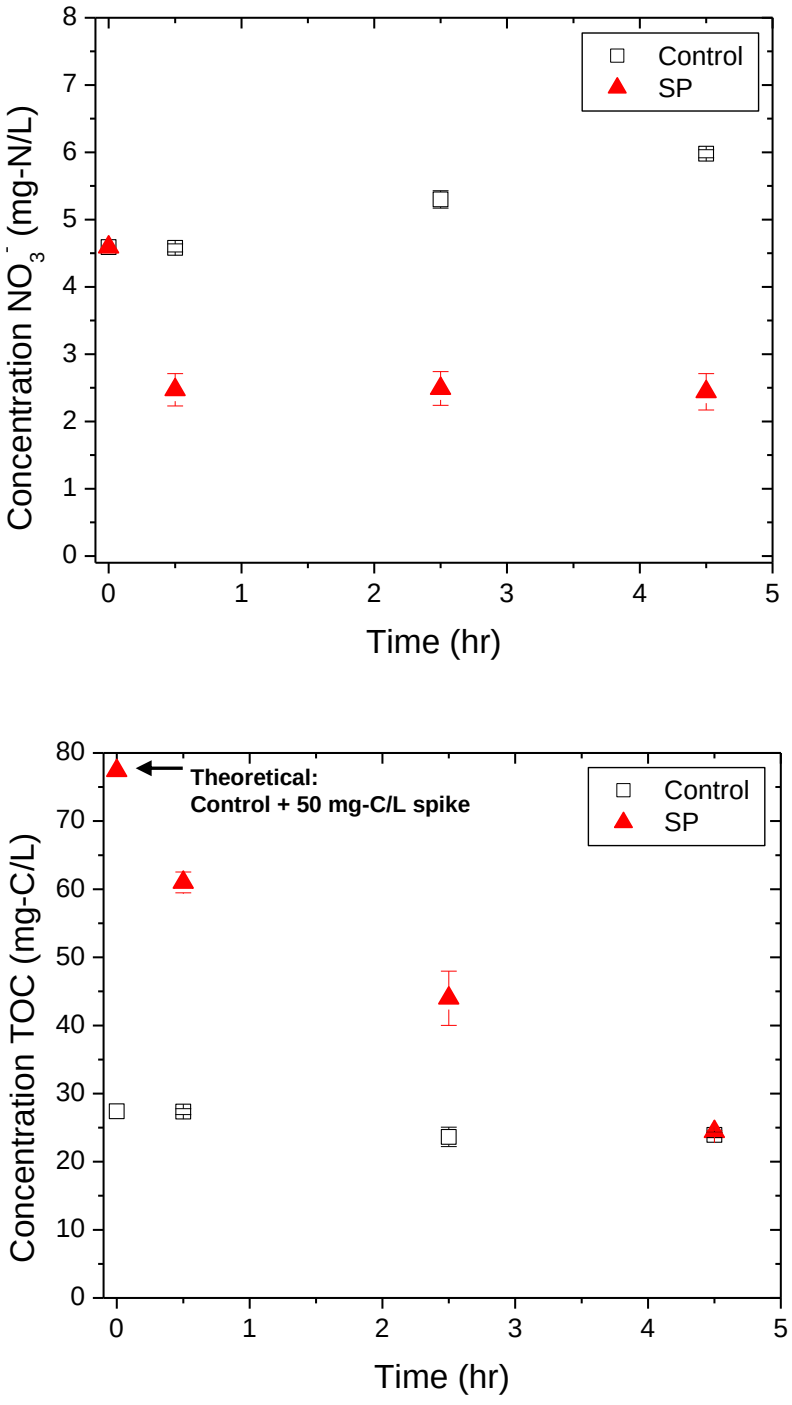

Figure 10. Concentration of a) NO_3^--N and b) TOC as a function of time in an aerobic environment batch experiment, Samples taken from a membrane bioreactor and spiked with 133 mg/L of sodium propionate (SP), equivalent to 50 mg-C/L, are compared to membrane bioreactor control samples.

A reduction in TOC concentration of approximately 37 mg/L for the SP samples after 4.5 hr indicates the biodegradability of the added organic carbon compared with the control samples, which only dropped approximately 3 mg/L (Figure 10b). The slight drop in TOC in the control samples is likely because the more biodegradable organic carbon degrades in the anoxic reactor of the MBR prior to entering the aerobic reactor, where the less biodegradable carbons remain. After 4.5 hr, the TOC concentration in both the controls and the SP samples were equal at approximately 24 mg/L, indicating complete removal of sodium propionate. Samples taken at 24 hr and 48 hr confirmed that the TOC concentrations in the controls and in the SP samples were still 24 mg/L, indicating that only more recalcitrant carbons remained in the samples. The rapid aerobic degradation of the sodium propionate demonstrates the likelihood that any additional sodium propionate entering the bioreactor (and not being utilized during anoxic denitrification) will be easily degraded in an aerobic environment.

4.6 Replenishment cost

The costs per liter to replenish the salts lost due to reverse salt flux during FO and salt passage during RO are given in Table 6. Also included is the total cost, which reflects the sum of salt loss during both the FO and RO processes. The costs for NaCl and $MgCl_2$, determined by Achilli et al. [5], were also included for comparison. Overall, magnesium acetate had the lowest FO replenishment costs because of its very low J_s/J_w value. Sodium formate had the highest replenishment costs due to the high unit cost and high J_s/J_w value. For the organic ionic draw solutions, sodium acetate and sodium propionate

had the lowest RO costs because they have the lowest unit costs. Magnesium acetate had higher RO replenishment costs due to the very high initial draw solution concentration required to achieve 1.4 MPa. All of the organic salts tested had higher RO replenishment costs than the inorganic draw solutes because of the higher unit costs. For total replenishment costs, sodium acetate and sodium propionate had the lowest of the organic salts tested, approximately equal to the total replenishment cost of $MgCl_2$ and slightly higher than the total replenishment cost of NaCl.

Table 6. Draw solution replenishment cost during operation. FO cost is the product of the specific reverse salt diffusion (J_s/J_w) and the draw solution unit cost ($/kg), and RO cost is the product of the RO permeate concentration and the draw solution unit cost. Total cost is the sum of the FO cost and the RO cost.

Draw Solution	**FO Cost** **$/L**	**RO Cost** **$/L**	**Total Cost** **$/L**
Sodium acetate	0.011	0.007	0.018
Sodium propionate	0.009	0.010	0.019
Magnesium acetate	0.005	0.024	0.029
Sodium formate	0.062	0.028	0.090
NaCl	0.011	0.002	0.013
$MgCl_2$	0.016	0.002	0.018

4.7 Future work

Chemical prediction could be added to the desktop screening process in future works. Possible chemical predictors are molar volume and degree of dissociation of the solutes. However, selection of chemical predictors (e.g., solute characteristics) that are readily available in the literature may be challenging. It is important to note that in this study, one factor affecting the performance of magnesium acetate as a draw solution was the unexpected conductivity-concentration relationship. Discoveries like this one, which

affected the water flux performance and the corresponding concentration polarization effects, may not be predicted simply by evaluating chemical predictors. Thus, the benefits of chemical predictions could eliminate unnecessary testing of less suitable draw solutions; however, laboratory testing may provide additional insights necessary for final selection.

5. CONCLUSIONS

Organic ionic salts were evaluated as draw solutions for OMBRs and evaluated based on several performance characteristics. Considering specific salt flux, reconcentration performance, biodegradation potential, and capital and replenishment costs, magnesium acetate and sodium propionate were the best-performing organic ionic salts. Biological batch experiments with sodium propionate showed an increased rate of denitrification in an anoxic environment when compared to control samples with no sodium propionate added. Partial degradation of nitrate also occurred in an aerobic environment when the sodium propionate was present. In addition, the biodegradability of sodium propionate in aerobic conditions was confirmed by observation of a reduction in the organic carbon concentration with time. The diffusion coefficient of each draw solution was also found using a method requiring only a characterized membrane. The replenishment costs of the organic draw solutions were slightly higher than leading inorganics; however, their efficient performance, biodegradation potential, and ability to facilitate denitrification make organic ionic salt draw solutions highly suitable for OMBR systems.

References

[1] T.Y. Cath, A.E. Childress, M. Elimelech, Forward osmosis: Principles, applications, and recent developments, J. Membr. Sci., 281 (2006) 70-87.
[2] A. Achilli, T.Y. Cath, E.A. Marchand, A.E. Childress, The forward osmosis membrane bioreactor: A low fouling alternative to MBR processes, Desalination, 239 (2009) 10-21.
[3] J.R. McCutcheon, R.L. McGinnis, M. Elimelech, A novel ammonia-carbon dioxide forward (direct) osmosis desalination process, Desalination, 174 (2005) 1-11.
[4] M.M. Ling, T.-S. Chung, Desalination process using super hydrophilic nanoparticles via forward osmosis integrated with ultrafiltration regeneration, Desalination, (2011) 194-202.
[5] A. Achilli, T.Y. Cath, A.E. Childress, Selection of inorganic-based draw solutions for forward osmosis applications, J. Membr. Sci., 364 (2010) 233-241.
[6] T.Y. Cath, V.D. Adams, A.E. Childress, Membrane contactor processes for wastewater reclamation in space. II. Combined direct osmosis, osmotic distillation, and membrane distillation for treatment of metabolic wastewater, J. Membr. Sci., 257 (2005) 111-119.
[7] R.W. Holloway, A.E. Childress, K.E. Dennett, T.Y. Cath, Forward osmosis for concentration of anaerobic digester centrate, Water Res., 41 (2007) 4005-4014.
[8] C.R. Martinetti, A.E. Childress, T.Y. Cath, High recovery of concentrated RO brines using forward osmosis and membrane distillation, J. Membr. Sci., 331 (2009) 31-39.
[9] S. Zou, Y. Gu, D. Xiao, C.Y. Tang, The role of physical and chemical parameters on forward osmosis membrane fouling during algae separation, J. Membr. Sci., 366 (2011) 356-362.
[10] N.Y. Yip, A. Tiraferri, W.A. Phillip, J.D. Schiffman, M. Elimelech, High Performance Thin-Film Composite Forward Osmosis Membrane, Environ. Sci. Technol., 44 (2010) 3812-3818.
[11] S.K. Yen, N.F.M. Haja, M. Su, Y. Wang, T.S. Chung, Study of draw solutes using 2-methylimidazole-based compounds in forward osmosis, J. Membr. Sci., 364 (2010) 242-252.
[12] Q. Ge, J. Su, G.L. Amy, T.S. Chung, Exploration of polyelectrolytes as draw solutes in forward osmosis porcesses, Water Res., 46 (2012) 1318-1326.
[13] N.H. Hancock, T.Y. Cath, Solute coupled diffusion in osmotically driven processes, Environ. Sci. Technol., 43 (2009) 6769–6775.
[14] D. Xiao, C. Tang, J. Zhang, W. Lay, R. Wang, A. Fane, Modeling salt accumulation in osmotic membrane bioreactors: Implications for FO membrane selection and system operation, J. Membr. Sci., (2011) 314-324.
[15] W. Lay, Q. Zhang, J. Zhang, D. McDougald, C. Tang, R. Wang, Y. Liu, A. Fane, Study of integration of forward osmosis and biological process: Membrane performance under elevated salt environment, Desalination, (2011) 1-8.
[16] W.J. Yap, J. Zhang, W.C.L. Lay, B. Cao, A.G. Fane, Y. Liu, State of the art of osmotic membrane bioreactors for water reclamation, in: Bioresource Technology, 2012.

[17] A. Alturki, J. McDonald, S.J. Khan, F.I. Hai, W.E. Price, L.D. Nghiem, Performance of a novel osmotic membrane bioreactor (OMBR) system: Flux stability and removal of trace organics, Bioresource Technology, 113 (2012).
[18] J. Zhang, W. Loong, S. Chou, C. Tang, R. Wang, A.G. Fane, Membrane biofouling and scaling in forward osmosis membrane bioreactor, J. Membr. Sci., 403-404 (2012) 8-14.
[19] E.R. Cornelissen, D. Harmsen, K.F.d. Korte, C.J. Ruiken, J. Qin, Membrane fouling and process performance of forward osmosis membranes on activated sludge, J. Membr. Sci., 319 (2008) 158-168.
[20] H. Zhang, M. Yanjie, J. Tao, Z. Guangyi, Y. Fenglin, Influence of activated sludge properties on flux behavior in osmosis membrane bioreactor (OMBR), J. Membr. Sci., 390-391 (2011) 270-276.
[21] J. Qin, M.H. Oo, G. Tao, E.R. Cornelissen, C.J. Ruiken, K.F.d. Korte, L.P. Wessels, K.A. Kekre, Optimization of operating conditions in forward osmosis for osmotic membrane bioreactor, Open Chem. Eng. J., 3 (2009) 27-32.
[22] O. Lefebvre, R. Moletta, Treatment of organic pollution in industrial saline wastewater: a literature review, Water Res., 40 (2006) 3671-3682.
[23] J. Shen, R. He, W. Han, X. Sun, J. Li, L. Wang, Biological denitrification of high-nitrate wastewater in a modified anoxic/oxic-membrane biorector (A/O-MBR), J. Hazard. Mater., 172 (2009) 595-600.
[24] S.W. Oa, G. Kim, Y. Kim, Determination of electron donors by comparing reaction rates for in situ bioremediation of nitrate-contaminated groundwater, Journal of Environmental Science and Health Part A, 41 (2006) 2359-2372.
[25] M. Islam, N. George, J. Zhu, N. Chowdhury, Impact of carbon to nitrogen ratio on nutrient removal in a liquid-solid circulating fluidized bed bioreactor (LSCFB), Process Biochemistry, 44 (2009) 578-583.
[26] M. Mulder, Basic principles of membrane technology, Kluver Academic Publishers, Dordrecht, The Netherlands, 1991.
[27] C.B. Ersu, S.K. Ong, E. Arslankaya, Y.W. Lee, Impact of solids retention time on biological nutrient removal performance of membrane bioreactor, Water Res., 44 (2010) 3192-3202.
[28] Metcalf, Eddy, Wastewater Engineering: Treatment and Reuse, Fourth ed., McGraw-Hill Professional, New York, 2003.
[29] C. Visvanathan, R. Aim, K. Parameshwaran, Membrane separation bioreactor for wastewater treatment, Critical Reviews in Environmental Science and Technology, 30 (2000) 1-48.
[30] J.R. McCutcheon, M. Elimelech, Influence of concentrative and dilutive internal concentration polarization on flux behavior in forward osmosis, J. Membr. Sci., 284 (2006) 237-247.
[31] A. Achilli, T.Y. Cath, A.E. Childress, Power generation with pressure retarded osmosis: an experimental and theoretical investigation, J. Membr. Sci., 343 (2009) 42-52.
[32] S. Ben-Yaakov, Diffusion of sea water ions-I. Diffusion of sea water into a dilute solution, Geochim. Cosmochim. Acta, 36 (1972) 1395-1406.

[33] A. Bonnier, A. Korganoff, The determination of dispersion coefficients in non-homogeneous media in problems of salt water contamination of fresh ground water, J. Hydrol., 16 (1972) 39-47.
[34] B. Csoka, G. Nagy, Determination of diffusion coefficient in gel and in aqueous solutions using scanning electrochemical microscopy, J. Biochem. Biophys. Methods, 61 (2004) 57-67.
[35] W.D. Williams, K.E. Sherwood, Definition and measurement of salinity in salt lakes, Int. J. Salt Lake Res., 3 (1994) 53-63.
[36] S. Zhao, L. Zou, Relating solution physicochemical properties to internal concentration polarization in forward osmosis, J. Membr. Sci., 379 (2011) 459-467.
[37] W.A. Phillip, J.S. Yong, M. Elimelech, Reverse draw solute permeation in forward osmosis: modeling and experiments, Environ. Sci. Technol., 44 (2010) 5170-5176.